Electromagnetic form factors and the proton radius

Jeremy Green

NIC, DESY, Zeuthen

Advances in Lattice Gauge Theory 2019
CERN, July 23, 2019

Outline

1. Nucleon form factors
2. Lattice QCD: standard methods
3. Direct methods for radii and magnetic moment
4. Outlook

Electromagnetic (vector) form factors

Elastic ep scattering cross section depends on the strength of the coupling of a proton to a current.

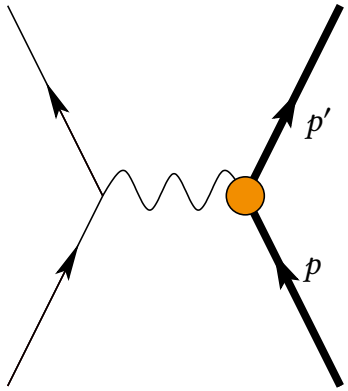

$Q^2 = -(p' - p)^2$

$$\langle p' | V_\mu^q | p \rangle = \bar{u}(p') \left[\gamma_\mu F_1^q(Q^2) + \frac{i\sigma_{\mu\nu}(p' - p)^\nu}{2m_p} F_2^q(Q^2) \right] u(p),$$

where $V_\mu^q = \bar{q}\gamma_\mu q$.

Electric and magnetic form factors:

$$G_E^q(Q^2) = F_1^q(Q^2) - \frac{Q^2}{(2m_p)^2} F_2^q(Q^2), \quad G_M^q(Q^2) = F_1^q(Q^2) + F_2^q(Q^2).$$

For a photon, weight quarks with their charges:

$$G_{E,M}^\gamma \equiv \tfrac{2}{3} G_{E,M}^u - \tfrac{1}{3} G_{E,M}^d - \tfrac{1}{3} G_{E,M}^s + \dots$$

Electromagnetic form factors: nonrelativistic

In the Breit frame ($\vec{p}' = -\vec{p} = \vec{q}/2$):

$$G_E(Q^2) \sim \rho_{\text{em}}, \qquad G_M(Q^2) \sim \vec{J}_{\text{em}}.$$

Non-relativistically, this motivates the definition of a charge density:

$$\rho_{\text{NR}}(\vec{r}^2) = \int \frac{d^3\vec{q}}{(2\pi)^3} e^{i\vec{q}\cdot\vec{r}} G_E(\vec{q}^2).$$

Integrating the density yields

$$\int d^3\vec{r}\, \rho_{\text{NR}}(\vec{r}^2) = G_E(0), \qquad \int d^3\vec{r}\, \vec{r}^2 \rho_{\text{NR}}(\vec{r}^2) = -6G_E'(0).$$

At $Q^2 = 0$, we get the charge and magnetic moment of the proton, and the slopes define the mean-squared electric and magnetic radii:

$$G_E(Q^2) = 1 - \tfrac{1}{6}(r_E^2)^p Q^2 + O(Q^4)$$
$$G_M(Q^2) = \frac{\mu_p}{\mu_N}\left(1 - \tfrac{1}{6}(r_M^2)^p Q^2 + O(Q^4)\right)$$

EM form factors: relativistic interpretation

"Earthrise" photo taken by Apollo 8 astronauts.

- Photo has 4 ms exposure time.
- Image of Earth taken ~ 1 s before Moon.
- Farthest point of Earth viewed ~ 20 ms before nearest point.

We actually see things along the light cone rather than at fixed time.
Apply same light-front approach to the proton.
Then we get a 2d transverse charge density

$$\rho(\vec{b}^2) = \int \frac{d^2\vec{q}}{(2\pi)^2} e^{i\vec{q}\cdot\vec{b}} F_1(\vec{q}^2).$$

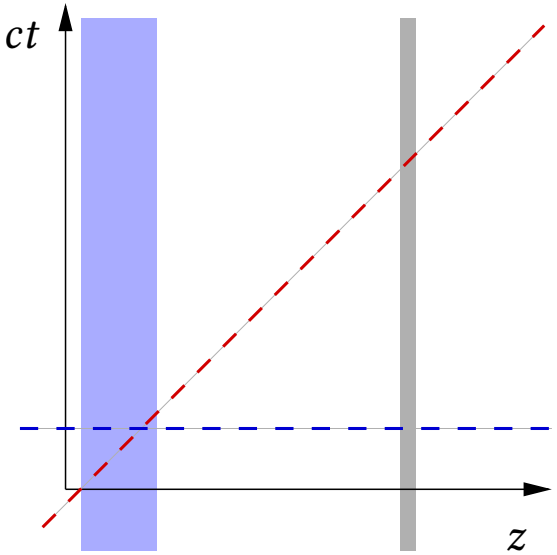

M. Diehl, Eur. Phys. J. C **25**, 223 [hep-ph/0205208],

M. Burkardt, Int. J. Mod. Phys. A **18**, 173 [hep-ph/0207047]

Electron-proton scattering

Electromagnetic form factors are studied using elastic scattering of an electron off a fixed proton target.

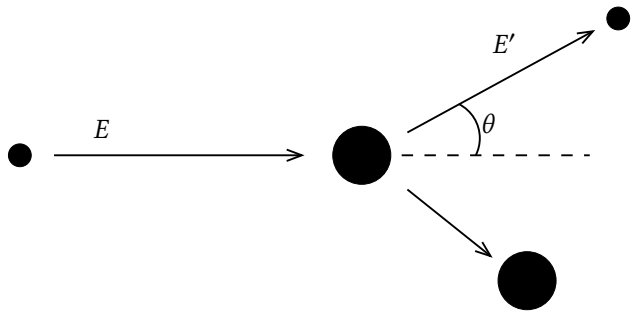

The differential scattering cross section behaves like

$$\frac{d\sigma}{d\Omega} \propto G_E(Q^2)^2 + \frac{\tau}{\epsilon} G_M(Q^2)^2, \qquad \tau = \frac{Q^2}{4m_p^2}, \quad \epsilon^{-1} = 1 + 2(2+\tau)\tan^2\frac{\theta}{2},$$

so that G_E and G_M can be measured in experiments (Rosenbluth separation).

- First experiments in 1950s (R. Hofstadter).
- Recent years: experiments in Mainz and JLab.
- Ongoing work studying low and high Q^2 regions.

Proton radius

How to measure r_E:

- From scattering experiments: measure $G_E(Q^2)$, then do curve fitting to find slope at $Q^2 = 0$.
- From atomic spectroscopy: the 2S–2P Lamb shift is sensitive to r_E. $\Delta E_{\text{finite size}} \propto r_E^2 m_e^3$

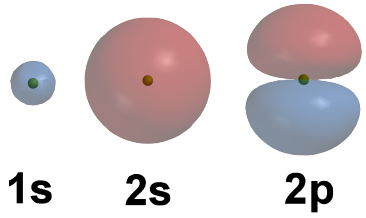

Muonic hydrogen spectrum is much more sensitive to r_E. This experiment led to proton radius puzzle.

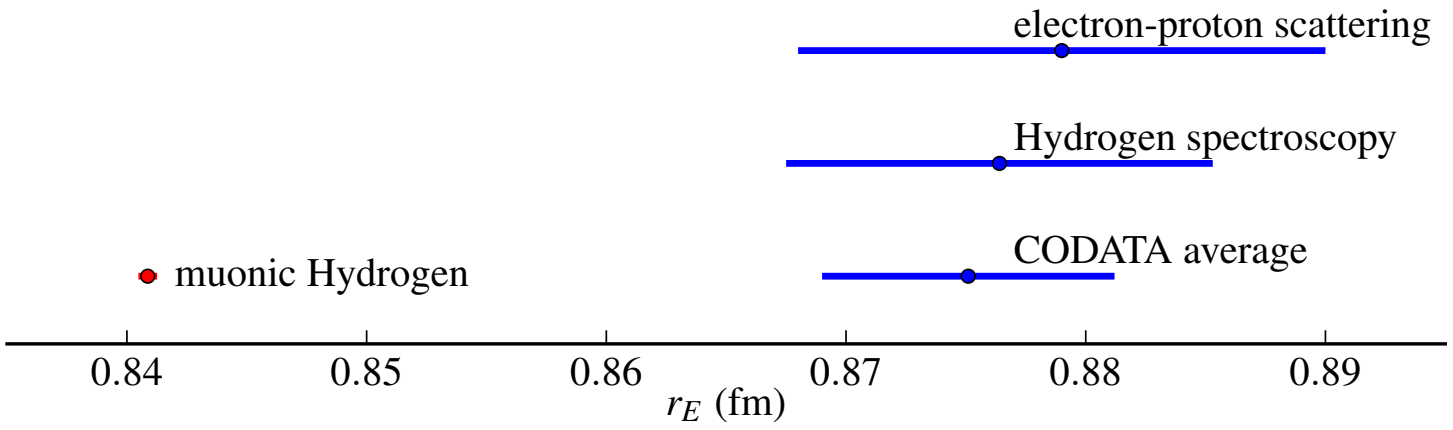

Proton radius: ongoing experiments

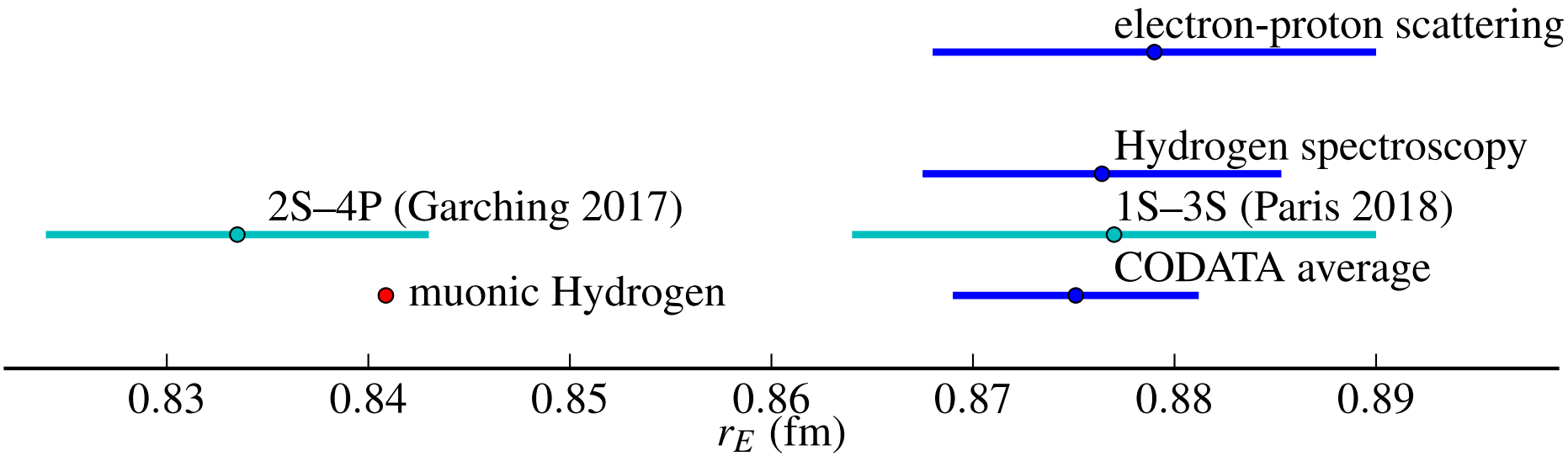

- New ep scattering experiments at low Q^2
  - Mainz ISR: $r_E = 0.870(28)$ fm M. Mihovilovič *et al.*, 1905.11182
  - JLab PRad: $r_E \sim 0.830(20)$ fm (preliminary: CERN Courier)
  - Tohoku: planned ULQ2 experiment using low beam energy (20–60 MeV).
- Muon-proton scattering
  - MUSE: $\mu^{\pm}p$, $e^{\pm}p$ scattering at PSI
  - COMPASS: proposed $\mu^{\pm}p$ experiment
- New hydrogen spectroscopy experiments: Garching, Paris, Toronto

Also note: analyses of scattering data based on dispersion relations yield small radius. M. A. Belushkin *et al.*, Phys. Rev. C **75**, 035202 (2007) [hep-ph/0608337]

An older puzzle: G_E/G_M at high Q^2

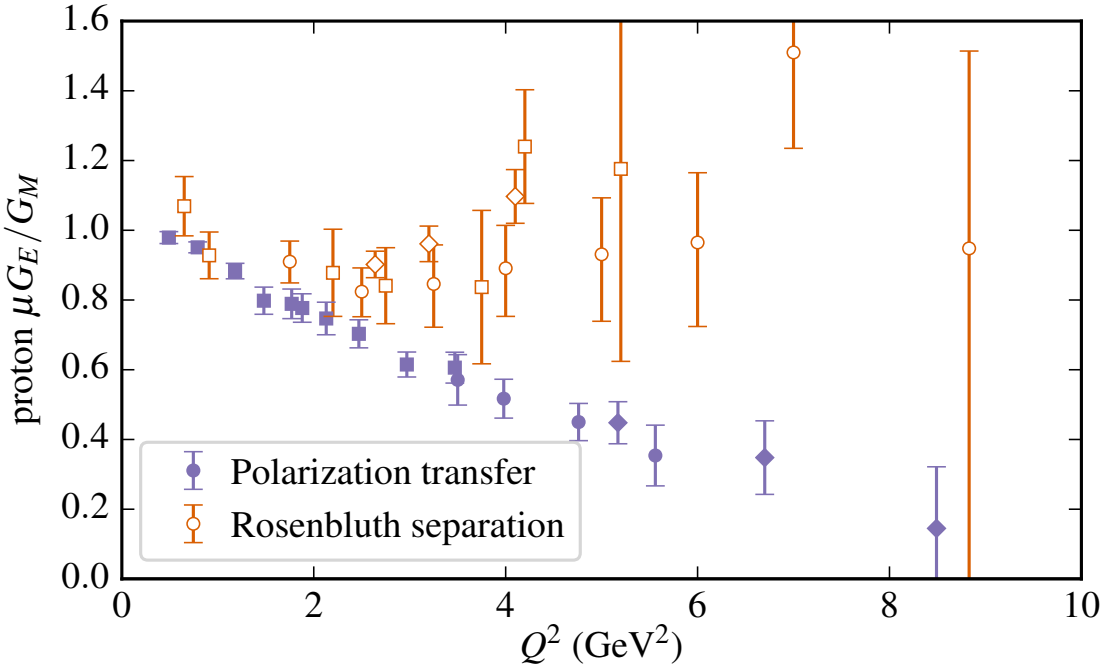

Polarization transfer, $\vec{e}p \to e\vec{p}$, gives a direct measurement of G_E/G_M.

Result disagreed with Rosenbluth separation.

Can be explained by contributions from two-photon exchange.

Explanation was tested via $\frac{\sigma(e^+p)}{\sigma(e^-p)}$, but not at high Q^2.

Flavour separation

Elastic ep scattering gives one flavour combination:

$$G^p_{E,M} = \tfrac{2}{3}G^u_{E,M} - \tfrac{1}{3}G^d_{E,M} - \tfrac{1}{3}G^s_{E,M} - \cdots$$

Separating out u, d, and s contributions requires two more independent combinations

1. Neutron electromagnetic form factors (assuming isospin): swap role of u and d. Obtained using ^{2}H or ^{3}He targets.
2. Contribution from Z exchange. Obtained from parity-violating asymmetry in elastic $\vec{e}p$ scattering.

Neutron-electron scattering length yields neutron charge radius:

$$b_{ne} = \frac{\alpha}{3} m_n r^2_{En}.$$

PDG average: $r^2_{En} = -0.1161(22)$.

Magnetic moment

Good benchmark observable: experimental situation is solid.

$\mu^p = 2.792\,847\,344\,62(82)\mu_N$ (0.3 ppb) PDG; G. Schneider *et al.*, Science **358**, 1081–1084 (2017)

$\mu^n = -1.913\,042\,73(45)\mu_N$ (0.2 ppm) CODATA; G. L. Greene *et al.*, Phys. Rev. D **20**, 2139 (1979)

Nuclear magneton: $\mu_N = \dfrac{e}{2m_p}$

Magnetic moment

Good benchmark observable: experimental situation is solid.

$\mu^p = 2.792\,847\,344\,62(82)\mu_N$ (0.3 ppb) PDG; G. Schneider *et al.*, Science **358**, 1081–1084 (2017)

$\mu^n = -1.913\,042\,73(45)\mu_N$ (0.2 ppm) CODATA; G. L. Greene *et al.*, Phys. Rev. D **20**, 2139 (1979)

$\mu^s \approx -0.02\mu_N$ (LQCD)

Nuclear magneton: $\mu_N = \dfrac{e}{2m_p}$

Magnetic radius

No independent measurements of r_M: only elastic scattering data.

Proton: reanalysis using z expansion

G. Lee *et al.*, Phys. Rev. D **92**, 013013 (2015) [1505.01489]

$$r_{Mp} = 0.776(34)(17) \text{ Mainz data}$$
$$r_{Mp} = 0.914(35) \text{ world data excluding Mainz}$$

Neutron: PDG 2019 cites two analyses

$r_{Mn} = 0.89(3)$ z expansion Z. Epstein *et al.*, Phys. Rev. D **90**, 074027 (2014) [1407.5687]

$r_{Mn} = 0.862^{+9}_{-8}$ disp. rel. M. A. Belushkin *et al.*, Phys. Rev. C **75**, 035202 (2007) [hep-ph/0608337]

Need for physical pion mass

Pion cloud makes large contribution to isovector radii.

Heavy baryon ChPT: V. Bernard *et al.*, Nucl. Phys. B **388**, 315–345 (1992)

$$(r_1^2)^{p-n} = -\frac{1}{(4\pi F_\pi)^2}\left[1 + 7g_A^2 + (2 + 10g_A^2)\log\left(\frac{m_\pi}{\Lambda}\right) + 12B_{10}^r(\Lambda)\right]$$

$$\kappa^{p-n} = \kappa_0^{p-n} - \frac{g_A^2 m_\pi m_N}{4\pi F_\pi^2}$$

$$\kappa^{p-n}(r_2^2)^{p-n} = \frac{g_A^2 m_N}{8\pi F_\pi^2 m_\pi}$$

Isovector r_1^2 and r_2^2 diverge as $m_\pi \longrightarrow 0$.

Hadron correlation functions

Compute two-point and three-point functions, using interpolator χ and operator insertion $\mathcal{O}$. In simplest case:

$$
\begin{aligned}
C_{2\mathrm{pt}}(t) &\equiv \langle \chi(t)\chi^\dagger(0)\rangle \\
&= \sum_n |Z_n|^2 e^{-E_n t} \\
&\to |Z_0|^2 e^{-E_0 t}\left(1 + O(e^{-\Delta E t})\right), \\
&\text{where } Z_n = \langle \Omega|\chi|n\rangle,
\end{aligned}
$$

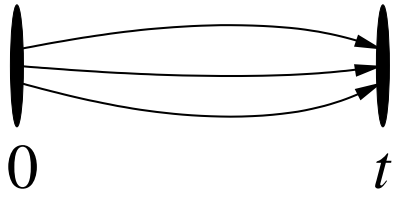

$$
\begin{aligned}
C_{3\mathrm{pt}}(\tau, T) &\equiv \langle \chi(T)\mathcal{O}(\tau)\chi^\dagger(0)\rangle \\
&= \sum_{n,n'} Z_{n'} Z_n^* \langle n'|\mathcal{O}|n\rangle e^{-E_n \tau} e^{-E_{n'}(T-\tau)} \\
&\to |Z_0|^2 \langle 0|\mathcal{O}|0\rangle e^{-E_0 T}\left(1 + O(e^{-\Delta E \tau}) + O(e^{-\Delta E (T-\tau)})\right)
\end{aligned}
$$

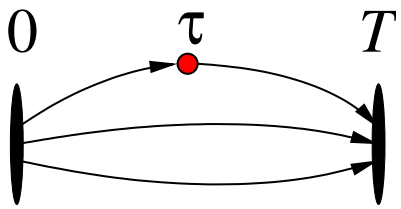

Hadron matrix elements

Ratio method

$$R(\tau, T) \equiv \frac{C_{3\text{pt}}(\tau, T)}{C_{2\text{pt}}(T)} = \langle 0|\mathcal{O}|0\rangle + O(e^{-\Delta E \tau}) + O(e^{-\Delta E (T-\tau)})$$

Midpoint yields $R(\frac{T}{2}, T) = \langle 0|\mathcal{O}|0\rangle + O(e^{-\Delta E T/2})$.

Summation method

$$S(T) \equiv \sum_{\tau} R(\tau, T), \qquad \frac{d}{dT} S(T) = \langle 0|\mathcal{O}|0\rangle + O(T e^{-\Delta E T})$$

Sum can be over all timeslices or from τ_0 to $T - \tau_0$.
Improved asymptotic behaviour noted in talks at Lattice 2010.

S. Capitani *et al.*, PoS LATTICE2010 147 [1011.1358]; J. Bulava *et al.*, *ibid.* 303 [1011.4393]

In practice noisier than ratio method at same T.

Two-point function: excited states

$$C_{2\mathrm{pt}}(t) = \langle \chi(t)\chi^\dagger(0)\rangle = \sum_n e^{-E_n t} \left|\langle n|\chi^\dagger|0\rangle\right|^2$$

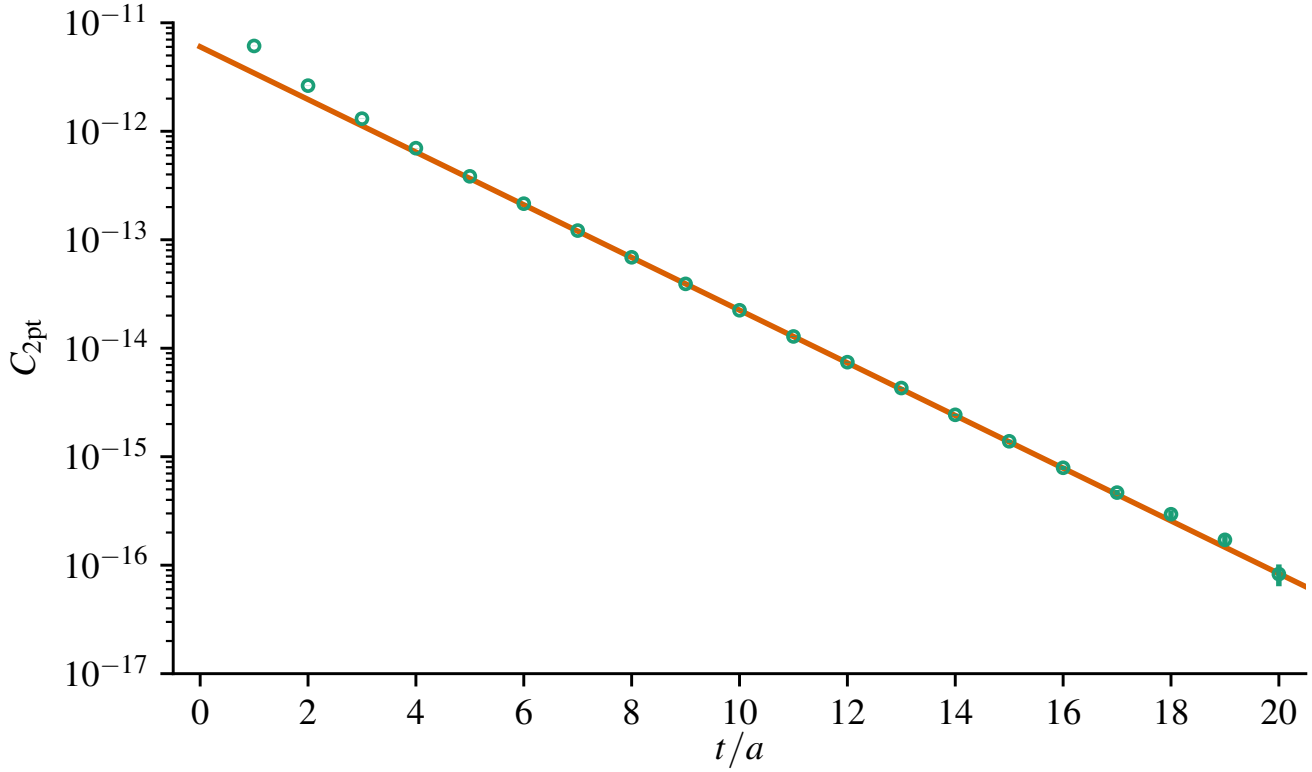

For a nucleon, the signal-to-noise asymptotically decays as $e^{-(m_N - \frac{3}{2}m_\pi)t}$.

Two-point function: excited states

$$C_{2\mathrm{pt}}(t) = \langle \chi(t)\chi^\dagger(0)\rangle = \sum_n e^{-E_n t} \left|\langle n|\chi^\dagger|0\rangle\right|^2$$

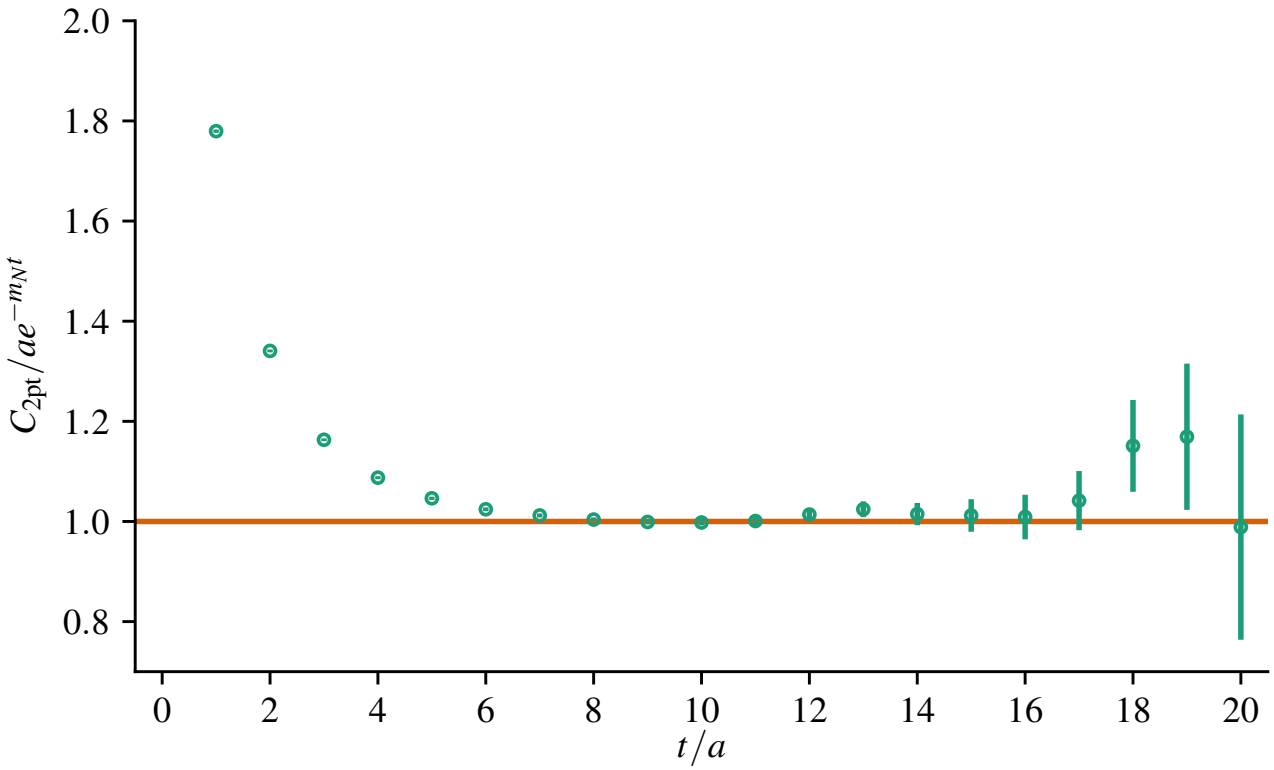

For a nucleon, the signal-to-noise asymptotically decays as $e^{-(m_N - \frac{3}{2}m_\pi)t}$.

Three-point function: excited states

$$\textit{ratio:} \quad R(T,\tau) = \frac{C_{3\mathrm{pt}}(T,\tau)}{C_{2\mathrm{pt}}(T)} \longrightarrow \langle N|\mathcal{O}|N\rangle$$

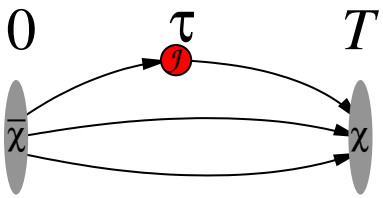

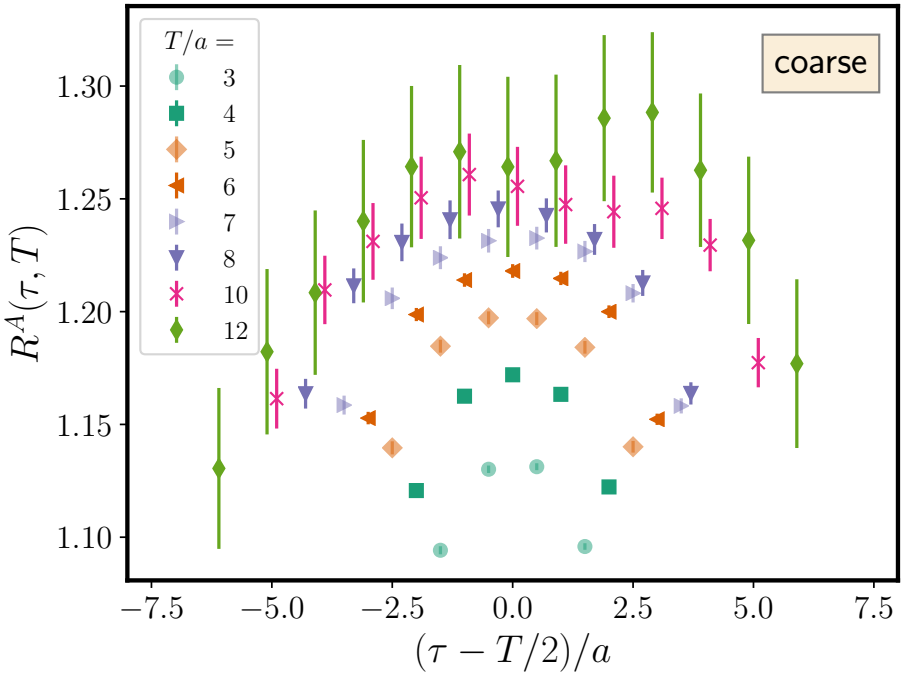

N. Hasan, JG, *et al.*, Phys. Rev. D **99**, 114505 (2019) [1903.06487]

Three-point function: excited states

$$\textit{ratio:} \quad R(T,\tau) = \frac{C_{3\mathrm{pt}}(T,\tau)}{C_{2\mathrm{pt}}(T)} \longrightarrow \langle N|\mathcal{O}|N\rangle$$

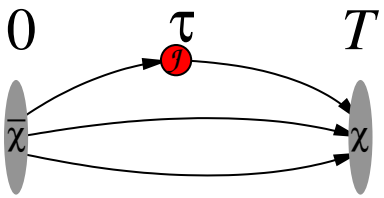

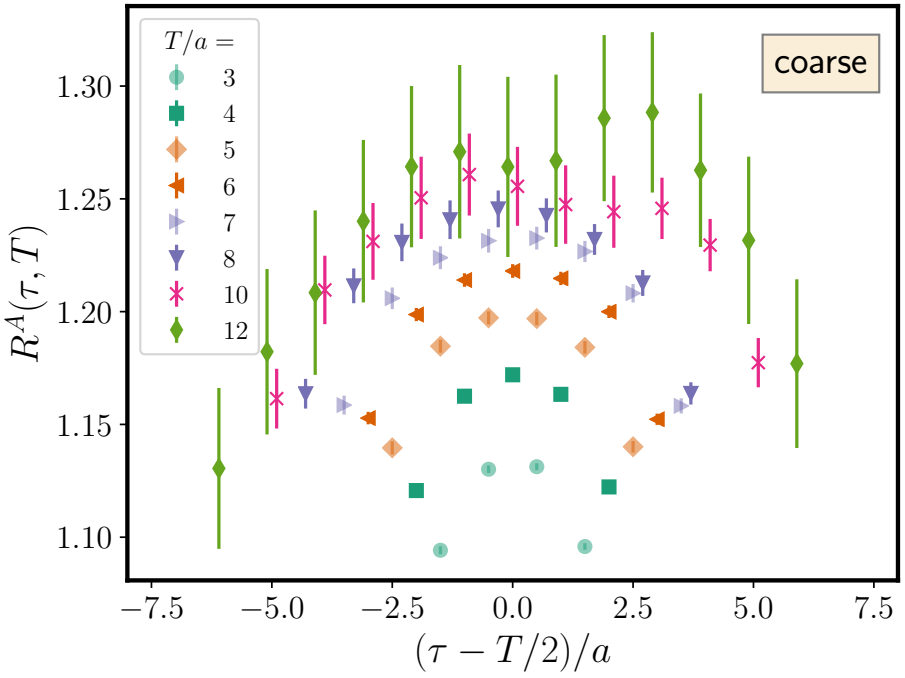

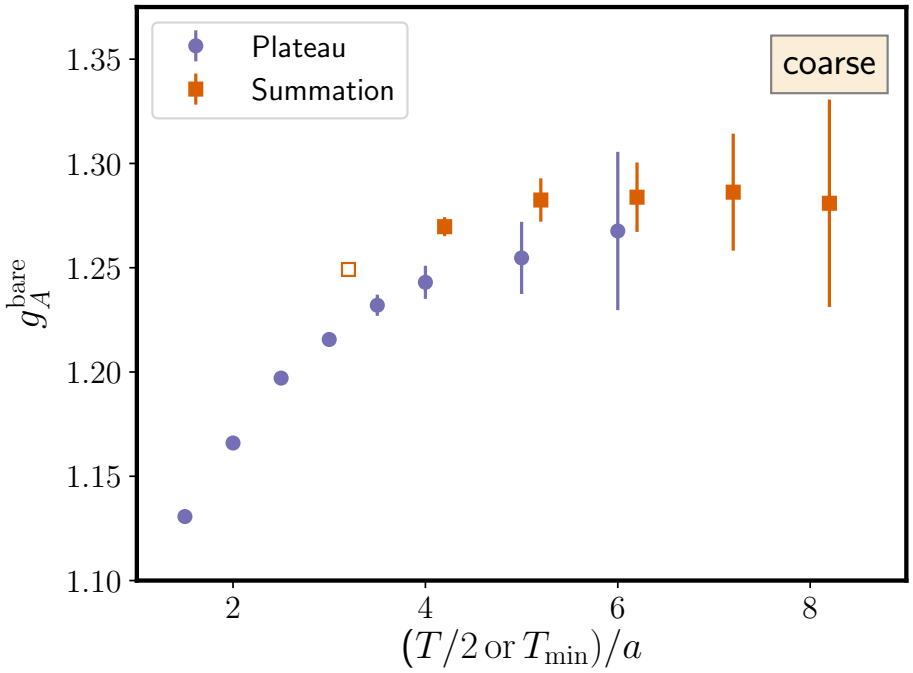

N. Hasan, JG, *et al.*, Phys. Rev. D **99**, 114505 (2019) [1903.06487]

Off-forward matrix elements

$$C^{\mathcal{O}}_{3\text{pt}}(\tau, T; \vec{p}, \vec{p}')$$
$$= \int d^3\vec{x} d^3\vec{y}\, e^{-i\vec{p}\cdot\vec{x}} e^{i(\vec{p}'-\vec{p})\cdot\vec{y}} \operatorname{Tr}\left[\Gamma_{\text{pol}} \langle \chi(\vec{x}, T)\mathcal{O}(\vec{y}, \tau)\bar{\chi}(0)\rangle\right]$$
$$\to \frac{Z(\vec{p})Z(\vec{p}')}{4E(\vec{p})E(\vec{p}')} e^{-E(\vec{p})\tau} e^{-E(\vec{p}')(T-\tau)} \sum_{s,s'} \bar{u}(p,s)\Gamma_{\text{pol}} u(p',s') \langle p', s'|\mathcal{O}|p, s\rangle \,.$$

Cancel overlaps and exponents using ratio:

$$R^{\mathcal{O}}(\tau, T; \vec{p}, \vec{p}') = \frac{C^{\mathcal{O}}_{3\text{pt}}(\tau, T; \vec{p}, \vec{p}')}{\sqrt{C_{2\text{pt}}(T, \vec{p})C_{2\text{pt}}(T, \vec{p}')}} \sqrt{\frac{C_{2\text{pt}}(\vec{p}, T-\tau)C_{2\text{pt}}(\vec{p}', \tau)}{C_{2\text{pt}}(\vec{p}', T-\tau)C_{2\text{pt}}(\vec{p}, \tau)}}$$

Extracting form factors

Matrix elements are linear combinations of form factors:

$$\langle p', s' | V_\mu | p, s \rangle = \bar{u}(p', s') \left[\gamma_\mu F_1(Q^2) + \frac{i\sigma_{\mu\nu}(p' - p)^\nu}{2m_p} F_2(Q^2) \right] u(p, s).$$

Gather matrix elements with the same Q^2:

- different μ
- different $\vec{p}, \vec{p}'$
- different polarization (i.e. s, s').

This gives a linear system of equations with two unknowns: $F_1(Q^2)$ and $F_2(Q^2)$.

Extracting form factors: rest frame

Consider states with $\vec{p}' = 0$ and spin in the $+\hat{z}$ direction.

$$\begin{aligned}
\Re(R^{V_i}) &\sim \epsilon_{ij3} p_j G_M(Q^2) \\
\Im(R^{V_i}) &\sim -p_i G_E(Q^2) \\
\Re(R^{V_4}) &\sim (m_N + E_N(\vec{p})) G_E(Q^2)
\end{aligned}$$

Most common approach: take $\Re(R^{V_i})$ and $\Re(R^{V_4})$.

Lattice results

Largest volume: $L = 10.8$ fm $\longrightarrow Q^2_{\text{min}} = 0.013$ GeV^2

E. Shintani *et al.* (PACS), Phys. Rev. D **99**, 014510 (2019) [1811.07292]

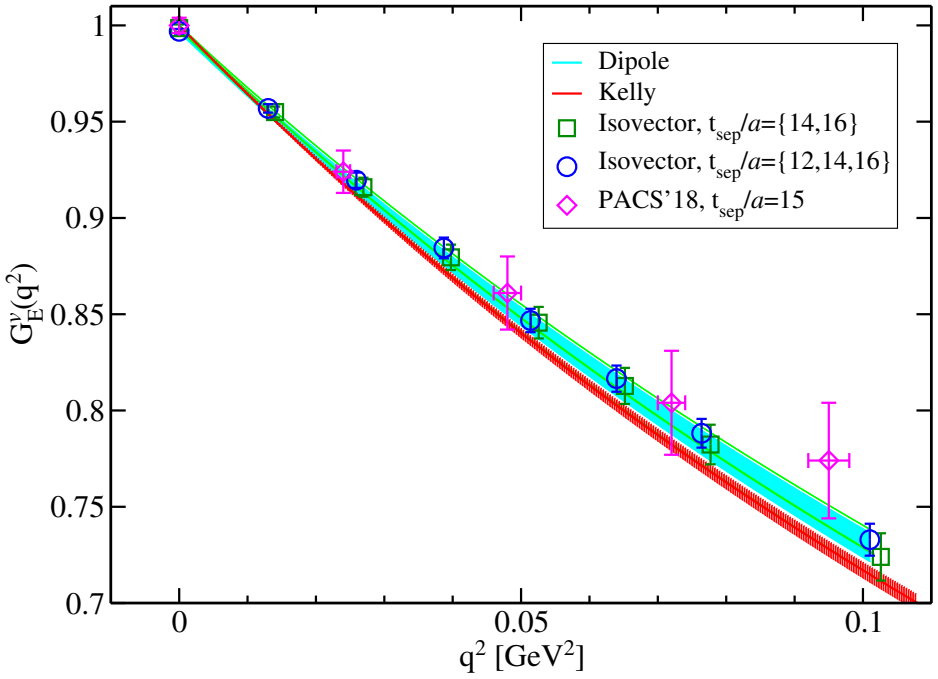

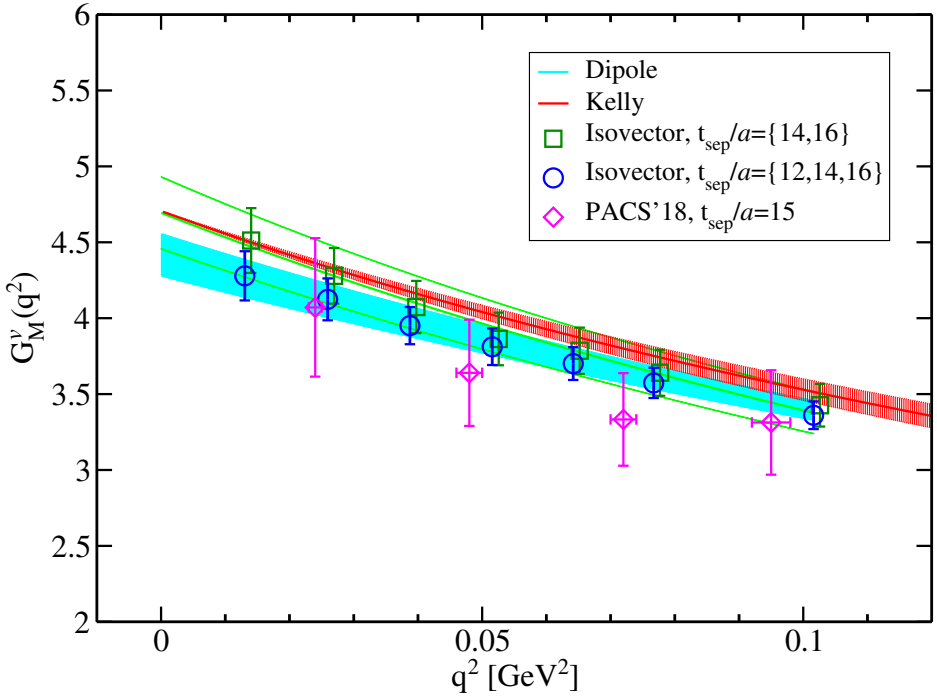

Lattice results

Largest volume: $L = 10.8$ fm $\longrightarrow Q^2_{\text{min}} = 0.013$ GeV^2

E. Shintani *et al.* (PACS), Phys. Rev. D **99**, 014510 (2019) [1811.07292]

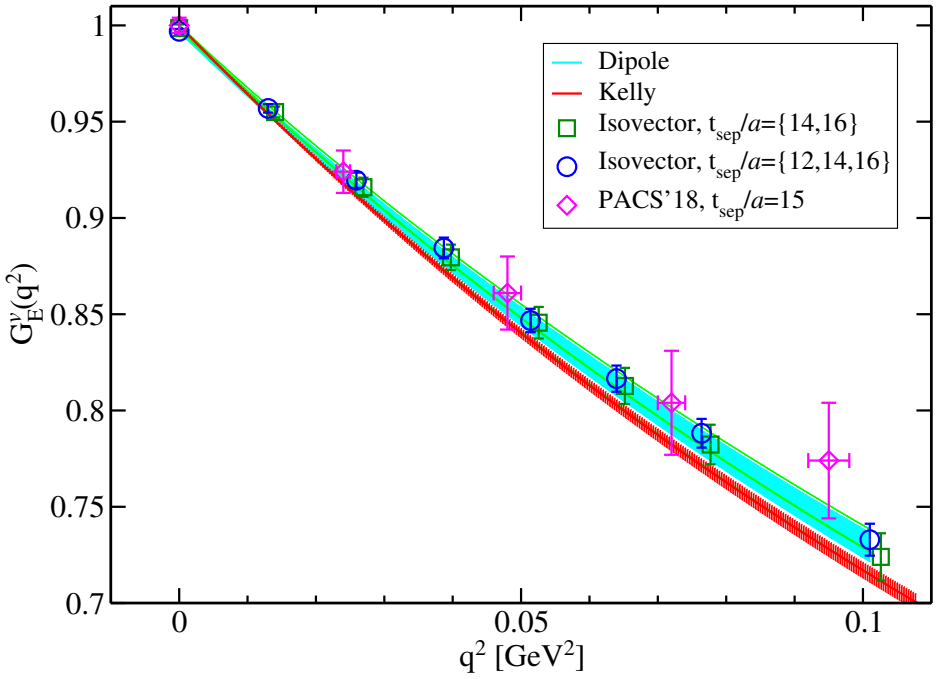

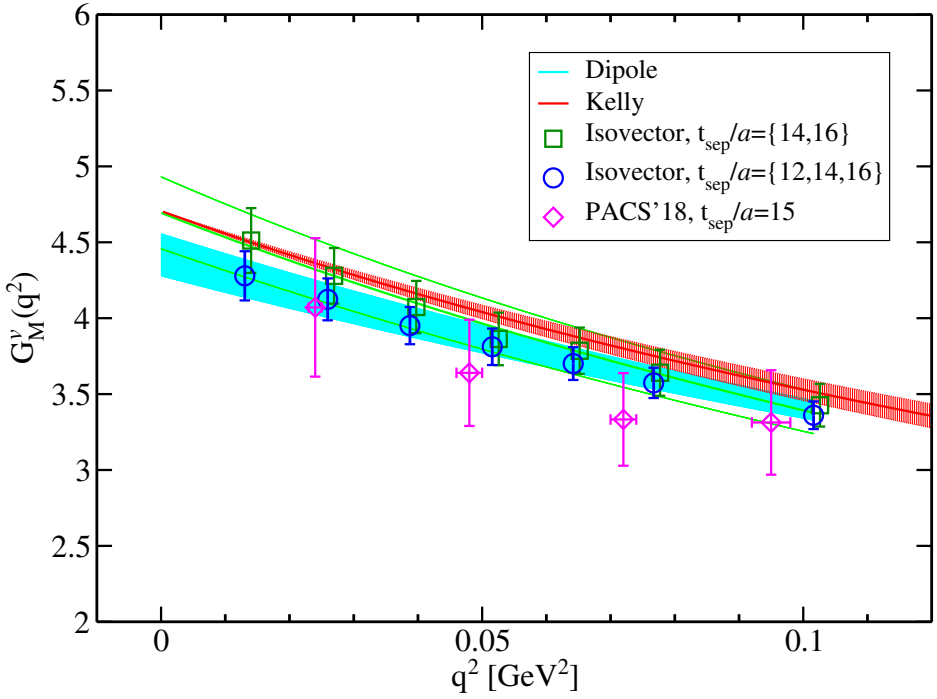

Minimum momentum transfer $Q^2_{\text{min}} \approx (\frac{2\pi}{L})^2$.

Lattice	L (fm)	Q^2_{min}(GeV^2)
LHPC 2010	2.7	0.203
LHPC 2014	5.6	0.048
PACS 2019	10.8	0.013

Lattice results

Largest volume: $L = 10.8$ fm $\longrightarrow Q^2_{\text{min}} = 0.013$ GeV^2

E. Shintani *et al.* (PACS), Phys. Rev. D **99**, 014510 (2019) [1811.07292]

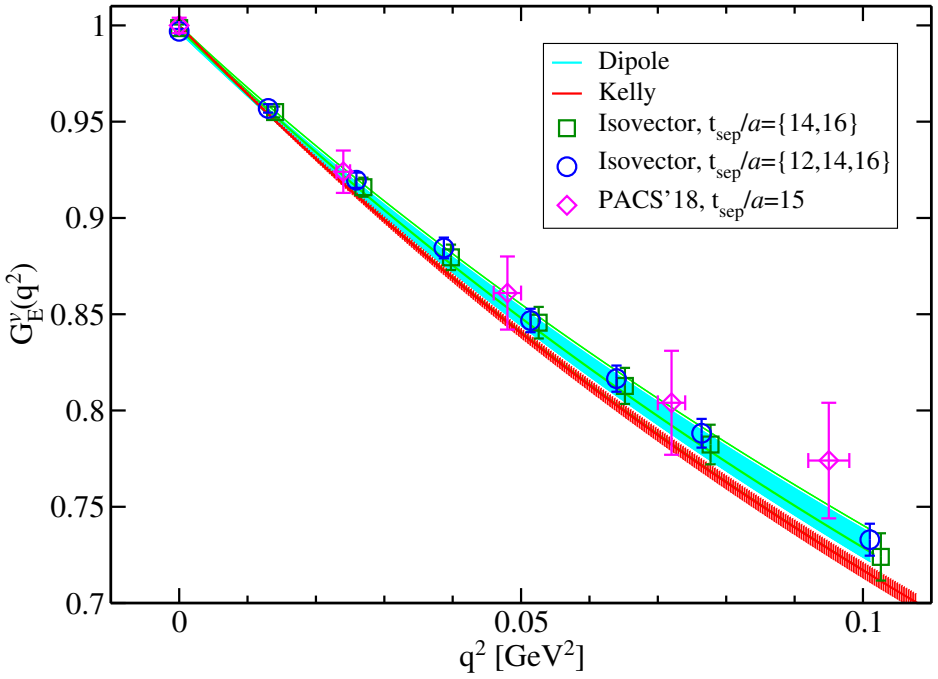

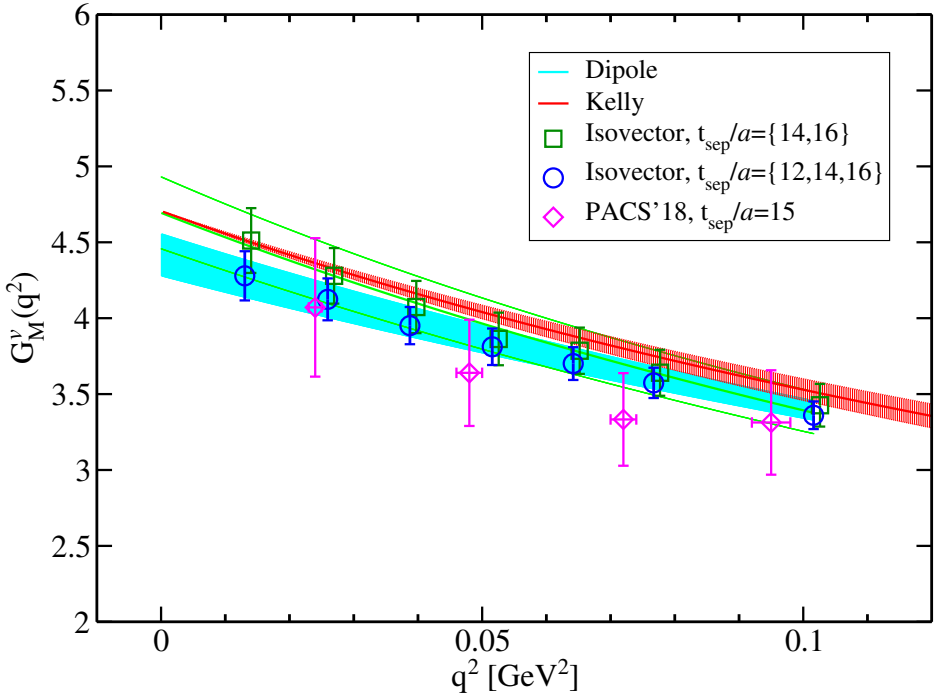

Minimum momentum transfer $Q^2_{\text{min}} \approx (\frac{2\pi}{L})^2$.

Lattice	L (fm)	Q^2_{min}(GeV^2)
LHPC 2010	2.7	0.203
LHPC 2014	5.6	0.048
PACS 2019	10.8	0.013

Experiment	Q^2_{min}(GeV^2)
Mainz 2014	0.003
Mainz ISR	0.001
JLab PRad	0.0002

Background field methods

Alternative approach with different systematics.
E.g. neutral hadron in uniform magnetic field: $E = m - \vec{\mu} \cdot \vec{B} + O(\vec{B}^2)$.

Background field methods

Alternative approach with different systematics.
E.g. neutral hadron in uniform magnetic field: $E = m - \vec{\mu} \cdot \vec{B} + O(\vec{B}^2)$.

Implement by modifying gauge links: $U_\mu(x) \longrightarrow e^{ie_q a A_\mu(x)} U_\mu(x)$.
For constant $\vec{B} = B\hat{z}$, can choose $A_\mu(x)$ such that with periodic boundary conditions,

$$e_q B = \frac{2\pi}{L^2} n, \quad n \in \mathbb{Z}.$$

Can study radii using spatially-varying $\vec{E}$ fields.
Z. Davoudi and W. Detmold, Phys. Rev. D **92**, 074506 (2015) [1507.01908]
Z. Davoudi and W. Detmold, Phys. Rev. D **93**, 014509 (2016) [1510.02444]

Direct calculation of μ (naïve attempt)

For spin $+\hat{z}$, we have $\Re[R^{V_x}(p\hat{y},\vec{0})] \sim pG_M(Q^2)$. Therefore

$$\frac{\mu}{\mu_N} = G_M(0) \sim \lim_{p\to 0}\frac{1}{p}\Re[R^{V_x}(p\hat{y},\vec{0})]$$
$$= \frac{\partial}{\partial p_y}\Re[R^{V_x}(\vec{p},\vec{0})]\Big|_{\vec{p}=0} = \frac{1}{C_{2\text{pt}}(T,\vec{0})}\frac{\partial}{\partial p_y}\Re\left[C^{V_x}_{3\text{pt}}(\tau,T;\vec{p},\vec{0})\right]\Big|_{\vec{p}=0},$$

where

$$\frac{\partial}{\partial p_y}C^{V_x}_{3\text{pt}}(\tau,T;\vec{p},\vec{0})\Big|_{\vec{p}=0} = \int d^3\vec{x}_1 d^3\vec{x}_2(-ix_{2y})\,\mathrm{Tr}\left[\Gamma_{\text{pol}}\langle\chi(\vec{x}_1,T)V_x(\vec{x}_2,\tau)\bar{\chi}(0)\rangle\right].$$

Failure of naïve approach

W. Wilcox, "Continuum moment equations on the lattice", Phys. Rev. D **66**, 017502 (2002) [hep-lat/0204024]

Need to choose finite-volume expression for the moment in y:

$$y \longrightarrow f_L(y) = \begin{cases} y & y < L/2 \\ 0 & y = L/2 \\ y - L & y > L/2 \end{cases}$$

Failure of naïve approach

W. Wilcox, "Continuum moment equations on the lattice", Phys. Rev. D **66**, 017502 (2002) [hep-lat/0204024]

Need to choose finite-volume expression for the moment in y:

$$y \longrightarrow f_L(y) = \begin{cases} y & y < L/2 \\ 0 & y = L/2 \\ y - L & y > L/2 \end{cases}$$

In finite volume, this can always be decomposed into Fourier modes:

$$f_L(y) = \sum_{n \in \mathbb{Z}} c_n e^{-ip_n y}, \quad p_n = \frac{2\pi}{L} n \implies c_n = \begin{cases} 0 & n = 0 \\ \frac{(-1)^n}{2i} \frac{L}{\pi n} & n \neq 0 \end{cases}$$

Failure of naïve approach

W. Wilcox, "Continuum moment equations on the lattice", Phys. Rev. D **66**, 017502 (2002) [hep-lat/0204024]

Need to choose finite-volume expression for the moment in y:

$$y \longrightarrow f_L(y) = \begin{cases} y & y < L/2 \\ 0 & y = L/2 \\ y - L & y > L/2 \end{cases}$$

In finite volume, this can always be decomposed into Fourier modes:

$$f_L(y) = \sum_{n \in \mathbb{Z}} c_n e^{-ip_n y}, \quad p_n = \frac{2\pi}{L} n \implies c_n = \begin{cases} 0 & n = 0 \\ \frac{(-1)^n}{2i} \frac{L}{\pi n} & n \neq 0 \end{cases}$$

At large τ, $C_{3\text{pt}}$ will be dominated by the lowest-lying initial states with energies $E_N(\vec{p} = p_n \hat{y})$, i.e. with $n = \pm 1$.

Failure of naïve approach

W. Wilcox, "Continuum moment equations on the lattice", Phys. Rev. D **66**, 017502 (2002) [hep-lat/0204024]

Need to choose finite-volume expression for the moment in y:

$$y \longrightarrow f_L(y) = \begin{cases} y & y < L/2 \\ 0 & y = L/2 \\ y - L & y > L/2 \end{cases}$$

In finite volume, this can always be decomposed into Fourier modes:

$$f_L(y) = \sum_{n \in \mathbb{Z}} c_n e^{-ip_n y}, \quad p_n = \frac{2\pi}{L} n \implies c_n = \begin{cases} 0 & n = 0 \\ \frac{(-1)^n}{2i} \frac{L}{\pi n} & n \neq 0 \end{cases}$$

At large τ, $C_{3\text{pt}}$ will be dominated by the lowest-lying initial states with energies $E_N(\vec{p} = p_n \hat{y})$, i.e. with $n = \pm 1$. Two problems:

1. The denominator $C_{2\text{pt}}(T, \vec{0})$ doesn't cancel $Z(\vec{p}) e^{-E_N(\vec{p})\tau}$.
2. We get matrix elements proportional to $G_M(Q^2_{\text{min}})$.
   Nothing new over standard approach.

Order of limits

Need to take $L \to \infty$ before $p \to 0$.
Correct order of limits for standard calculation:

$$\frac{\mu}{\mu_N} \propto \lim_{p\to 0} \lim_{L\to\infty} \lim_{\tau, T-\tau\to\infty} \frac{1}{p} \Re \left[R^{V_x}(\tau, T; p\hat{y}, \vec{0}) \right].$$

Order of limits

Need to take $L \to \infty$ before $p \to 0$.
Correct order of limits for standard calculation:

$$\frac{\mu}{\mu_N} \propto \lim_{p\to 0} \lim_{L\to\infty} \lim_{\tau, T-\tau\to\infty} \frac{1}{p} \Re \left[R^{V_x}(\tau, T; p\hat{y}, \vec{0}) \right].$$

Can postpone ground-state isolation:

$$\frac{\mu}{\mu_N} \propto \lim_{\tau, T-\tau\to\infty} \lim_{p\to 0} \lim_{L\to\infty} \frac{1}{p} \Re \left[R^{V_x}(\tau, T; p\hat{y}, \vec{0}) \right].$$

Order of limits

Need to take $L \to \infty$ before $p \to 0$.
Correct order of limits for standard calculation:

$$\frac{\mu}{\mu_N} \propto \lim_{p\to 0} \lim_{L\to\infty} \lim_{\tau, T-\tau\to\infty} \frac{1}{p} \Re \left[R^{V_x}(\tau, T; p\hat{y}, \vec{0}) \right].$$

Can postpone ground-state isolation:

$$\frac{\mu}{\mu_N} \propto \lim_{\tau, T-\tau\to\infty} \lim_{p\to 0} \lim_{L\to\infty} \frac{1}{p} \Re \left[R^{V_x}(\tau, T; p\hat{y}, \vec{0}) \right].$$

We can take finite-volume moments of a *correlator*:

$$\frac{\mu}{\mu_N} \propto \lim_{\tau, T-\tau\to\infty} \lim_{L\to\infty} \frac{\partial}{\partial p_y} \Re \left[R^{V_x}(\tau, T; \vec{p}, \vec{0}) \right] \Big|_{\vec{p}=0}.$$

This approach not currently being taken, but discussed in

C. Alexandrou *et al.* (ETMC), Phys. Rev. D **94**, 074508 (2016) [1605.07327].

Twisted boundary conditions

For $p_\mu = \frac{2\pi}{L_\mu} n_\mu$, $n_\mu \in \mathbb{Z}$, can absorb momentum into quark propagator:

$$e^{-ip\cdot(x-y)} D^{-1}(x, y; U) = D^{-1}(x, y; U^{(p)}), \quad U_\mu^{(p)}(x) = e^{iap_\mu} U_\mu(x).$$

Twisted boundary conditions

For $p_\mu = \frac{2\pi}{L_\mu} n_\mu$, $n_\mu \in \mathbb{Z}$, can absorb momentum into quark propagator:

$$e^{-ip\cdot(x-y)} D^{-1}(x, y; U) = D^{-1}(x, y; U^{(p)}), \quad U_\mu^{(p)}(x) = e^{iap_\mu} U_\mu(x).$$

For non-Fourier modes $p_\mu = \frac{1}{L_\mu}(2\pi n_\mu + \theta_\mu)$, using $U^{(p)}$ implies twisted boundary conditions

$$D^{-1}(x + L_\mu \hat{\mu}, y; U) = e^{i\theta_\mu} D^{-1}(x, y; U).$$

Twisted boundary conditions

For $p_\mu = \frac{2\pi}{L_\mu} n_\mu$, $n_\mu \in \mathbb{Z}$, can absorb momentum into quark propagator:

$$e^{-ip\cdot(x-y)} D^{-1}(x, y; U) = D^{-1}(x, y; U^{(p)}), \quad U_\mu^{(p)}(x) = e^{iap_\mu} U_\mu(x).$$

For non-Fourier modes $p_\mu = \frac{1}{L_\mu}(2\pi n_\mu + \theta_\mu)$, using $U^{(p)}$ implies twisted boundary conditions

$$D^{-1}(x + L_\mu \hat{\mu}, y; U) = e^{i\theta_\mu} D^{-1}(x, y; U).$$

Derivatives with respect to p can be evaluated exactly

G. M. de Divitiis, R. Petronzio, N. Tantalo, Phys. Lett. B **718**, 589–596 (2012) [1208.5914]

$$\frac{\partial D^{-1}}{\partial p_\mu} = -D^{-1} \frac{\partial D}{\partial p_\mu} D^{-1}$$

For Wilson-type fermions, $\frac{\partial D}{\partial p_\mu}$ amounts to an insertion of the conserved vector current.

Twisted boundary conditions: form factors

Need to absorb momentum into $D^{-1}(x, y)$ with $x \neq y$
$\implies$ can't use for disconnected diagrams. Equivalently, need flavor-changing vector current $\bar{q}_{\theta'}\gamma_\mu q_\theta$ with different twist angles $\theta' \neq \theta$.

Twisted boundary conditions: form factors

Need to absorb momentum into $D^{-1}(x, y)$ with $x \neq y$
$\implies$ can't use for disconnected diagrams. Equivalently, need flavor-changing vector current $\bar{q}_{\theta'}\gamma_\mu q_\theta$ with different twist angles $\theta' \neq \theta$.
Use *partially twisted* boundary conditions, i.e. only on valence quarks connected to current. Nonunitarity vanishes as $L \to \infty$.

Twisted boundary conditions: form factors

Need to absorb momentum into $D^{-1}(x, y)$ with $x \neq y$
$\implies$ can't use for disconnected diagrams. Equivalently, need flavor-changing vector current $\bar{q}_{\theta'}\gamma_\mu q_\theta$ with different twist angles $\theta' \neq \theta$.
Use *partially twisted* boundary conditions, i.e. only on valence quarks connected to current. Nonunitarity vanishes as $L \to \infty$.

Two applications:

1. Studying finite-volume effects. Twisted BC allows for the same momentum on different volumes.

Twisted boundary conditions: form factors

Need to absorb momentum into $D^{-1}(x, y)$ with $x \neq y$
$\implies$ can't use for disconnected diagrams. Equivalently, need flavor-changing vector current $\bar{q}_{\theta'}\gamma_\mu q_\theta$ with different twist angles $\theta' \neq \theta$.
Use *partially twisted* boundary conditions, i.e. only on valence quarks connected to current. Nonunitarity vanishes as $L \to \infty$.

Two applications:

1. Studying finite-volume effects. Twisted BC allows for the same momentum on different volumes.
2. Momentum derivatives at $\vec{p} = 0$.

$$\frac{\partial}{\partial p_j} \to \mu,$$

$$\frac{\partial^2}{\partial p_j^2} \text{ or } \frac{\partial^2}{\partial p_j' \partial p_j} \to r_E^2.$$

Lattice study: derivative method

Calculations at physical m_π using BMW 2HEX-clover action.
First version used $\frac{\partial}{\partial p_j}$ and $\frac{\partial^2}{\partial p_j^2}$
$\longrightarrow$ extra propagators shared for all source-sink separations.

N. Hasan, JG, *et al.*, Phys. Rev. D **97**, 034504 (2018) [1711.11385]

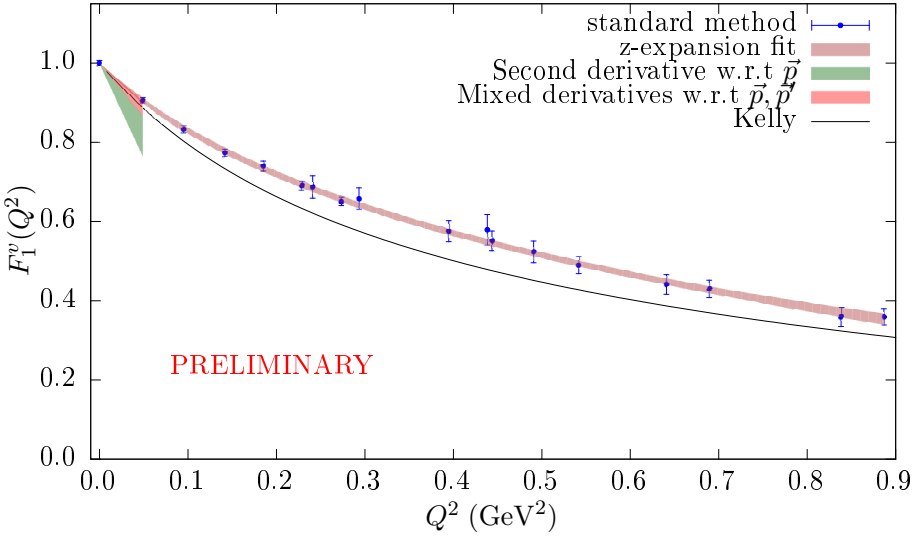

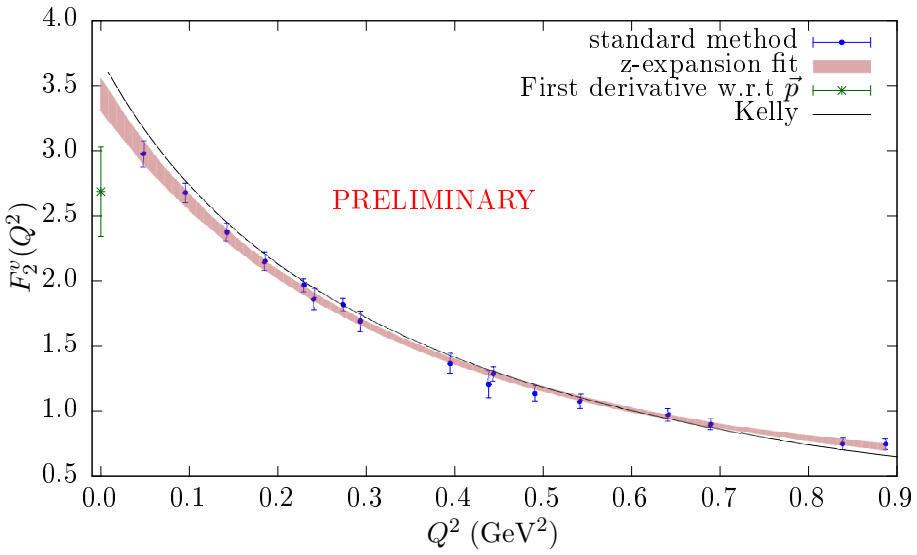

Revised approach also uses $\frac{\partial^2}{\partial p_j' \partial p_j}$
$\longrightarrow$ reduced statistical errors for r_E^2.

N. Hasan, talk at Lattice 2017

Finite-volume effects: ChPT

F.-J. Jiang and B. C. Tiburzi, *Flavor twisted boundary conditions and the nucleon vector current*, Phys. Rev. D **78**, 114505 (2008) [0810.1495]

- Heavy baryon partially quenched ChPT.
- Two sea quarks plus additional valence and ghost quarks with twisted BC.
- New unphysical baryon LEC g_1: equals $2g_A^{d,\text{conn}}$ in chiral limit.

E.g. for $\vec{p} = 0, \vec{p}' = p\hat{y}$:

$$\delta_L[G_M^{u-d}(Q^2)] = \frac{-2m_N}{f^2 p}(g_A^2 + g_A g_1)\mathcal{K}^2(m_\pi, \vec{p}, 0) + \frac{3m_N}{f^2}\int_0^1 dx\Big[g_A^2\mathcal{L}^{33}(m_\pi P_\pi, \vec{0}, \vec{p}, x\vec{p}, 0) + \frac{2}{9}g_{\Delta N}^2\mathcal{L}^{33}(m_\pi P_\pi, \vec{0}, \vec{p}, x\vec{p}, \Delta)\Big],$$

where $P_\pi = \sqrt{1 + x(1-x)p^2/m_\pi^2}$ and $\mathcal{K}^i$, $\mathcal{L}^{ij}$ are finite-volume functions.

Finite-volume effects from ChPT: isovector G_M

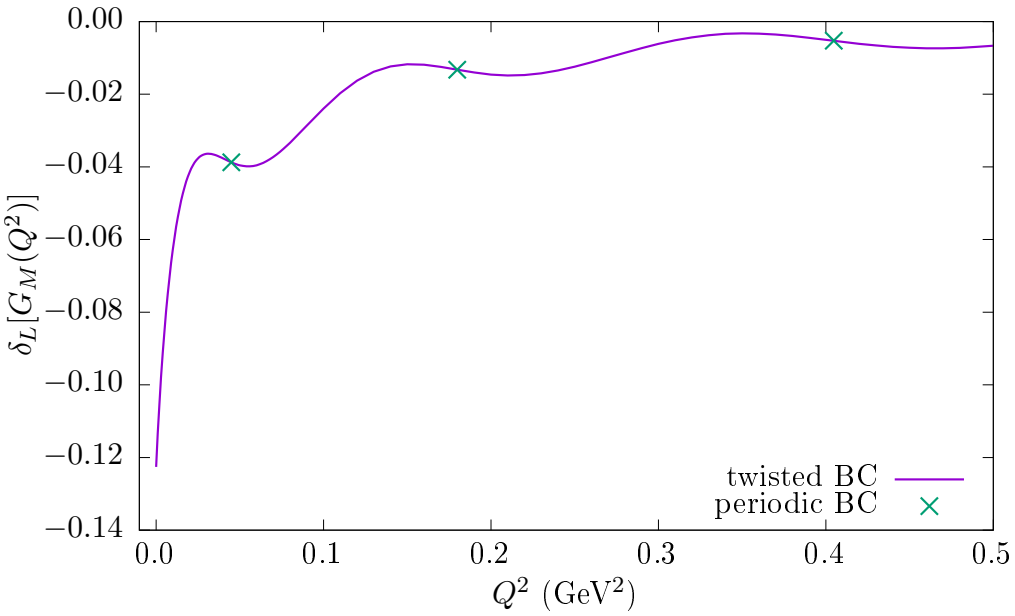

physical m_π, $m_\pi L = 4$

Derivative method:

$\delta_L[\mu/\mu_N] \to$
$-\frac{m_N}{\pi f^2}(2g_A^2 + g_A g_1) m_\pi e^{-m_\pi L}$.

Compare with

$\delta_L[g_A] \sim m_\pi^2 e^{-m_\pi L}/\sqrt{m_\pi L}$.

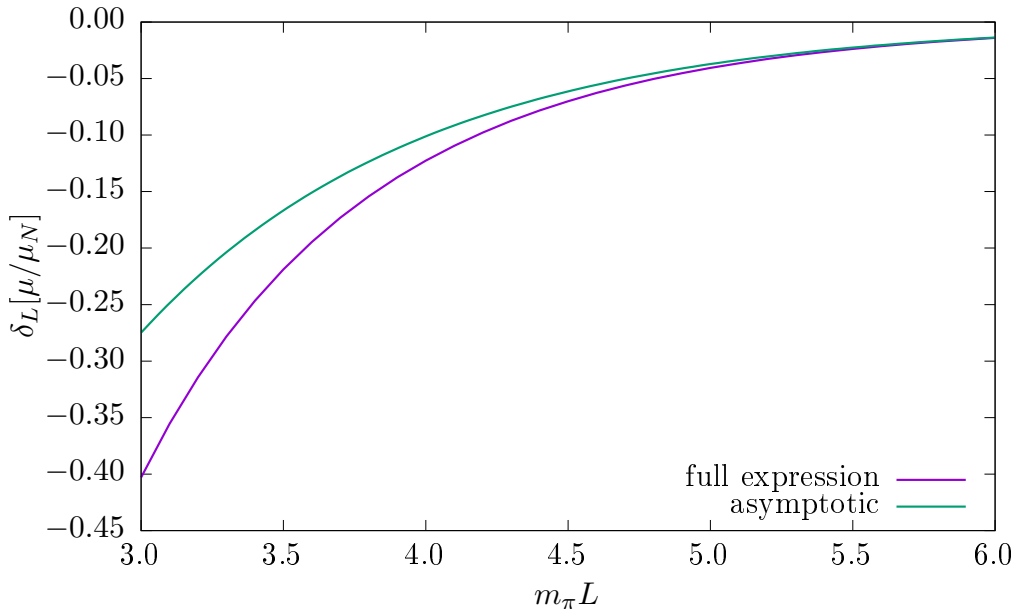

Finite-volume effects from ChPT: isovector G_E

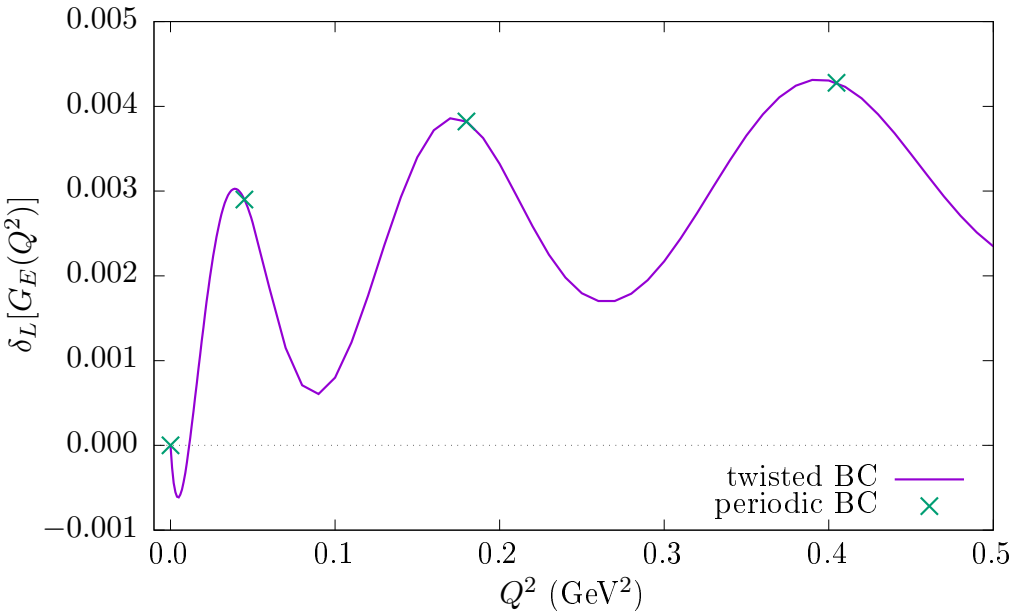

physical m_π, $m_\pi L = 4$

Derivative method:
$\delta_L[r_E^2] \sim (m_\pi L)^{3/2} e^{-m_\pi L}$.
Slow approach to asymptote;
better approx.: $(2/f^2)e^{-m_\pi L}$.

Compare with
$\delta_L[g_A] \sim m_\pi^2 e^{-m_\pi L}/\sqrt{m_\pi L}$.

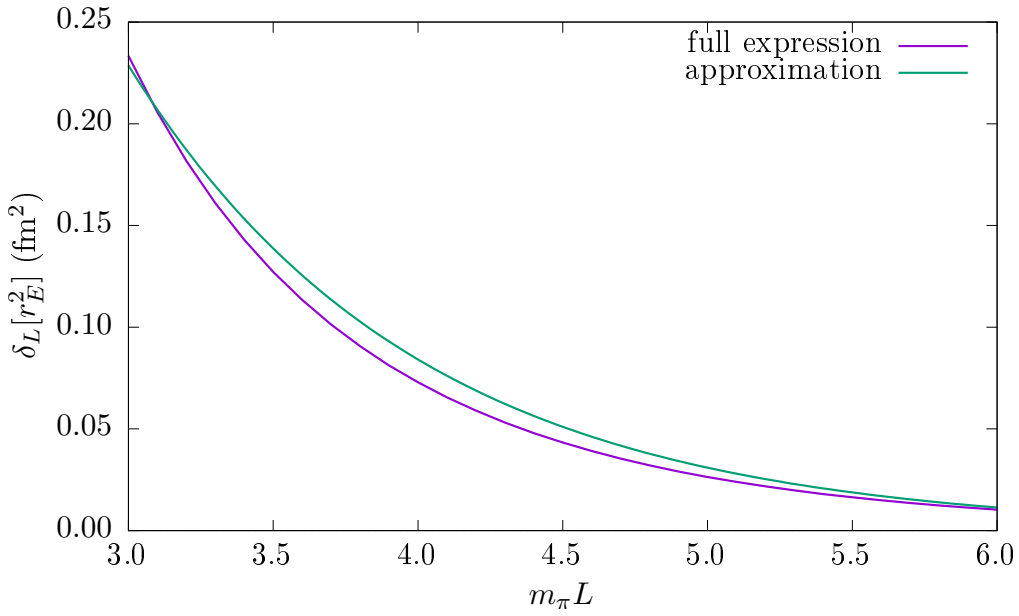

Lattice study: finite volume

Two ensembles with $m_\pi \approx 250$ MeV, $a = 0.116$ fm:

1. $32^3 \times 48$, $m_\pi L = 4.8$
2. $24^3 \times 48$, $m_\pi L = 3.6$, plus twisted BC to match momenta

Results are PRELIMINARY.

Lattice study: finite volume

Two ensembles with $m_\pi \approx 250$ MeV, $a = 0.116$ fm:

1. $32^3 \times 48$, $m_\pi L = 4.8$
2. $24^3 \times 48$, $m_\pi L = 3.6$, plus twisted BC to match momenta

Results are PRELIMINARY.

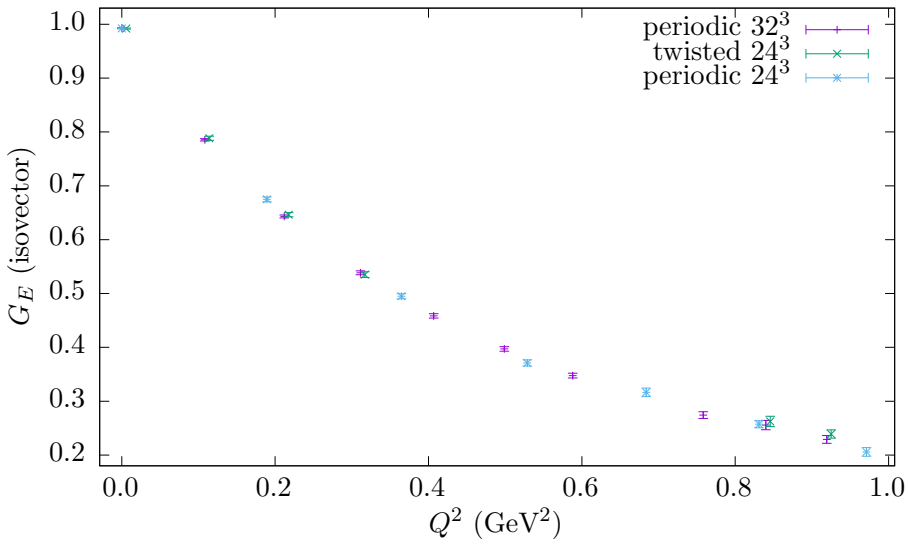

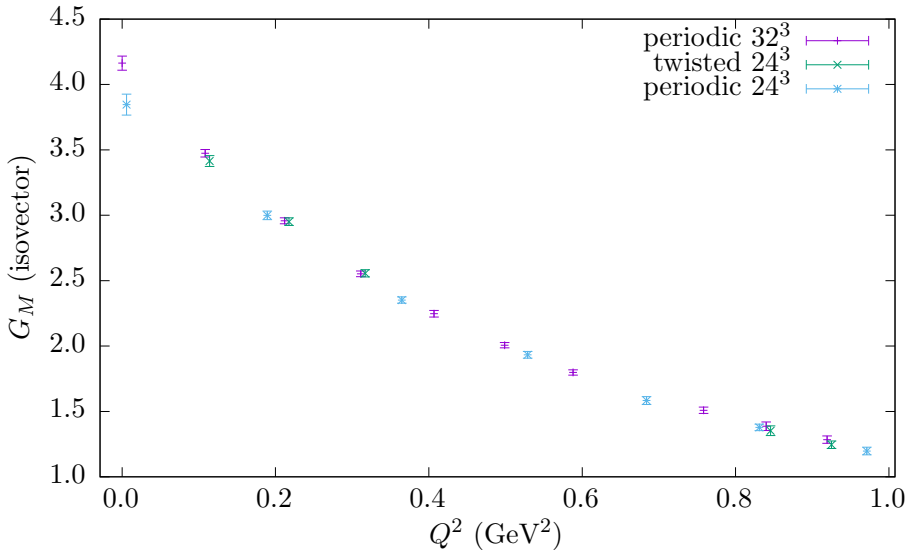

Lattice study: finite volume

Two ensembles with $m_\pi \approx 250$ MeV, $a = 0.116$ fm:

1. $32^3 \times 48$, $m_\pi L = 4.8$
2. $24^3 \times 48$, $m_\pi L = 3.6$, plus twisted BC to match momenta

Results are PRELIMINARY.

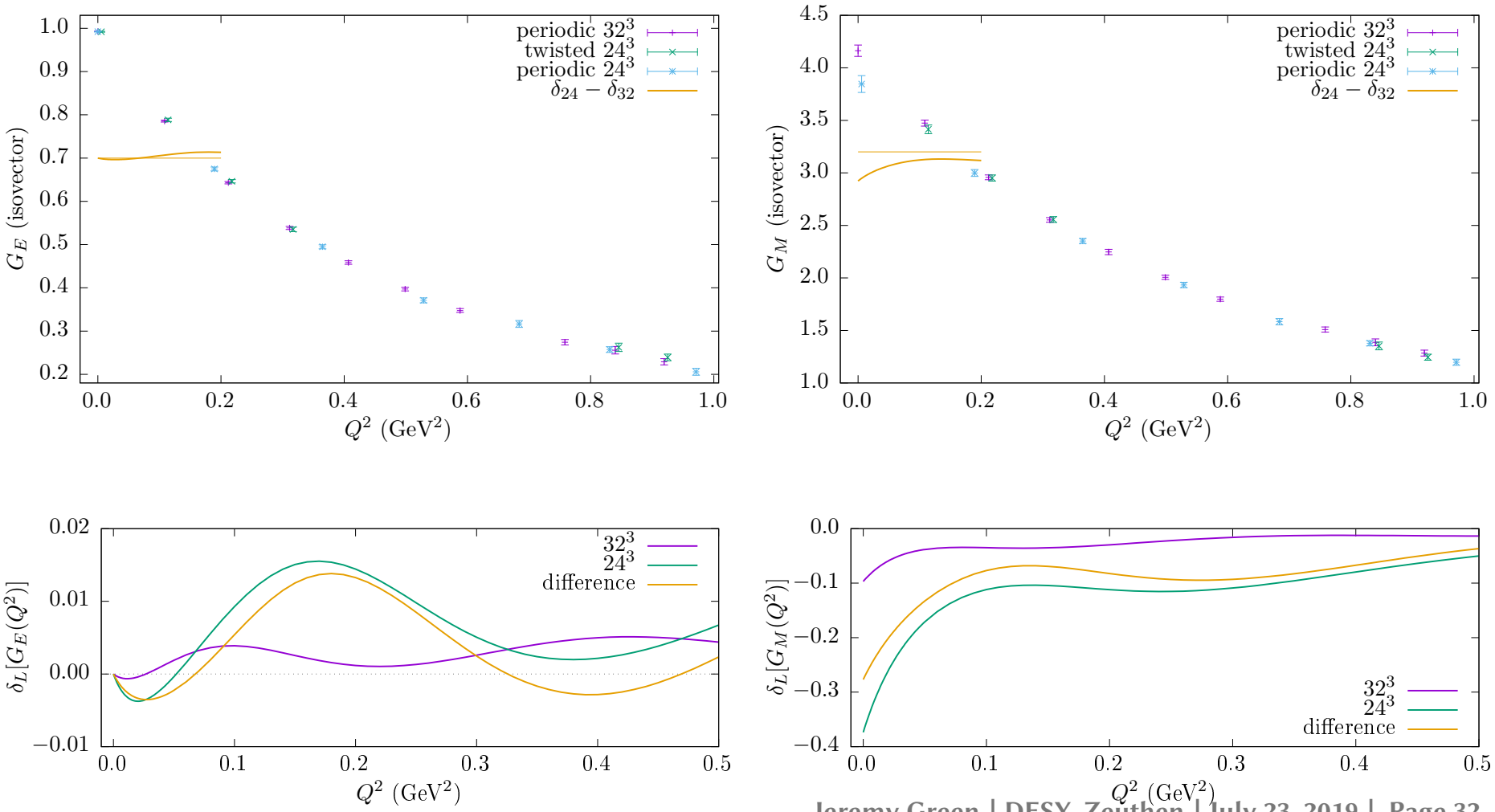

Lattice study: finite volume derivative method

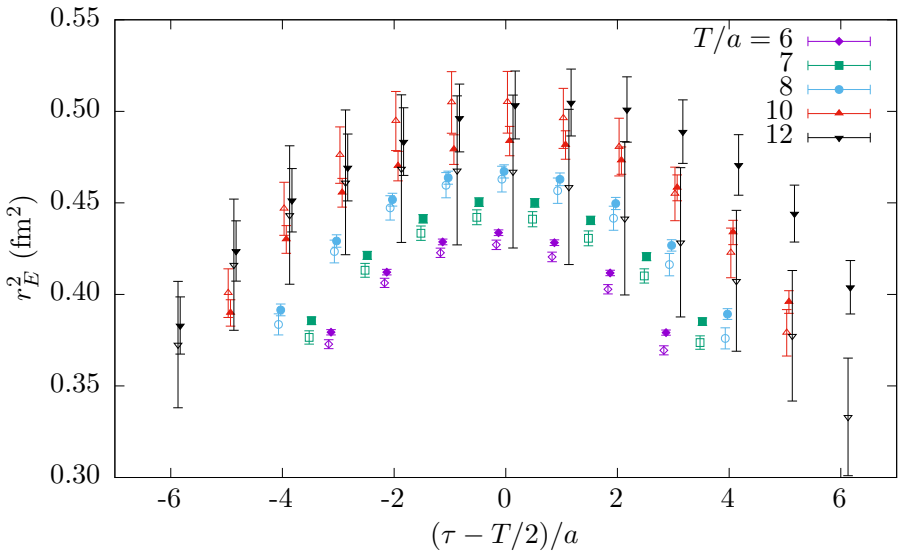

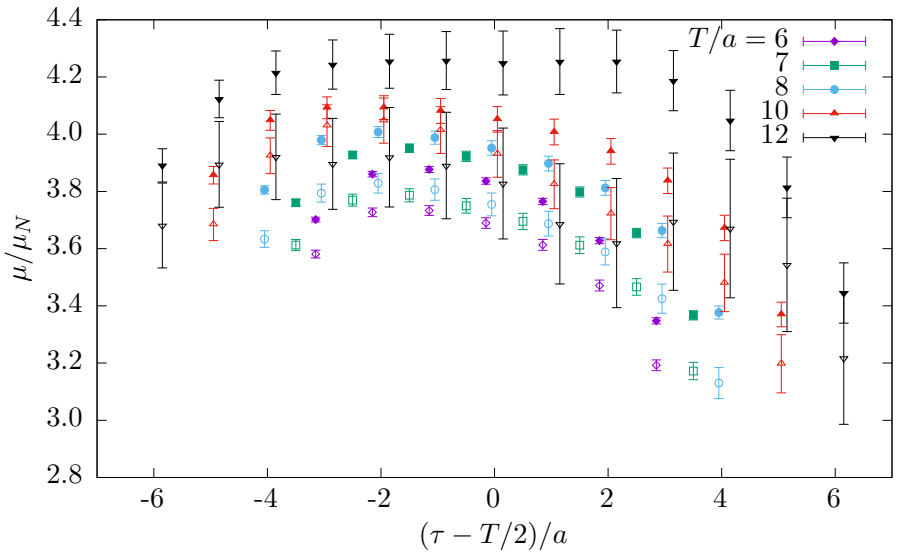

open symbols: 24^3
filled symbols: 32^3

$\sim -2\%$ effect for r_E^2; ChPT: $(r_E^2)_{24} - (r_E^2)_{32} = +0.076$ fm^2
$\sim -5\%$ effect for μ; ChPT: $\mu_{24} - \mu_{32} = -0.28$

Lattice study: finite volume derivative method

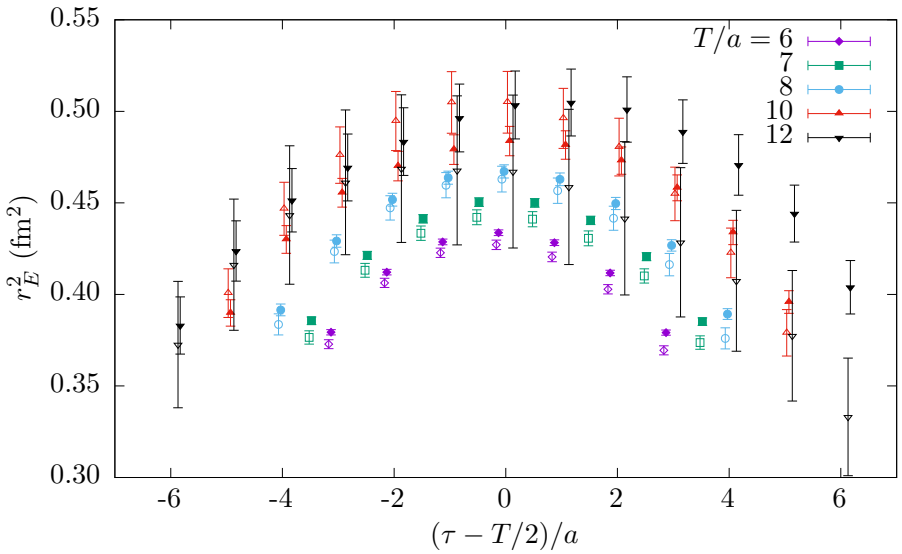

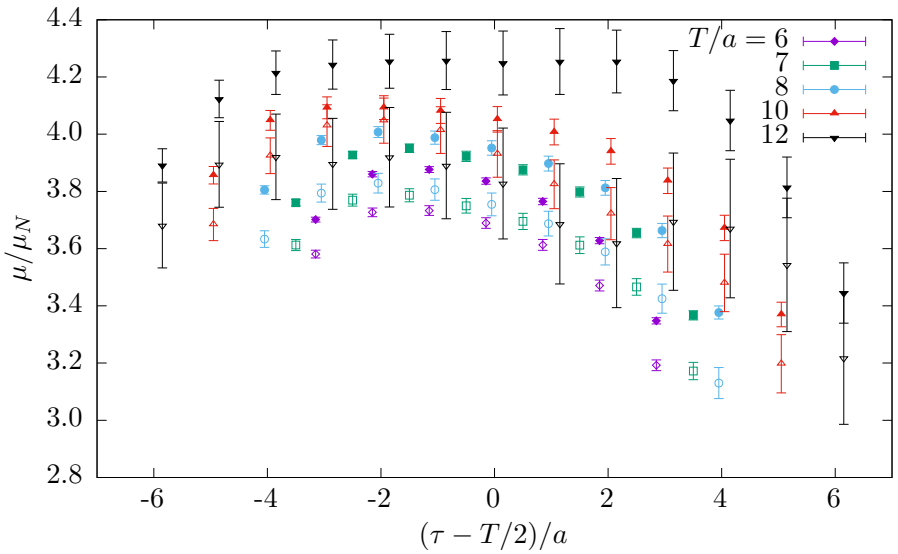

open symbols: 24^3
filled symbols: 32^3

$\sim -2\%$ effect for r_E^2; ChPT: $(r_E^2)_{24} - (r_E^2)_{32} = +0.076$ fm^2
$\sim -5\%$ effect for μ; ChPT: $\mu_{24} - \mu_{32} = -0.28$

Excited-state effects are significant!

Disconnected diagrams?

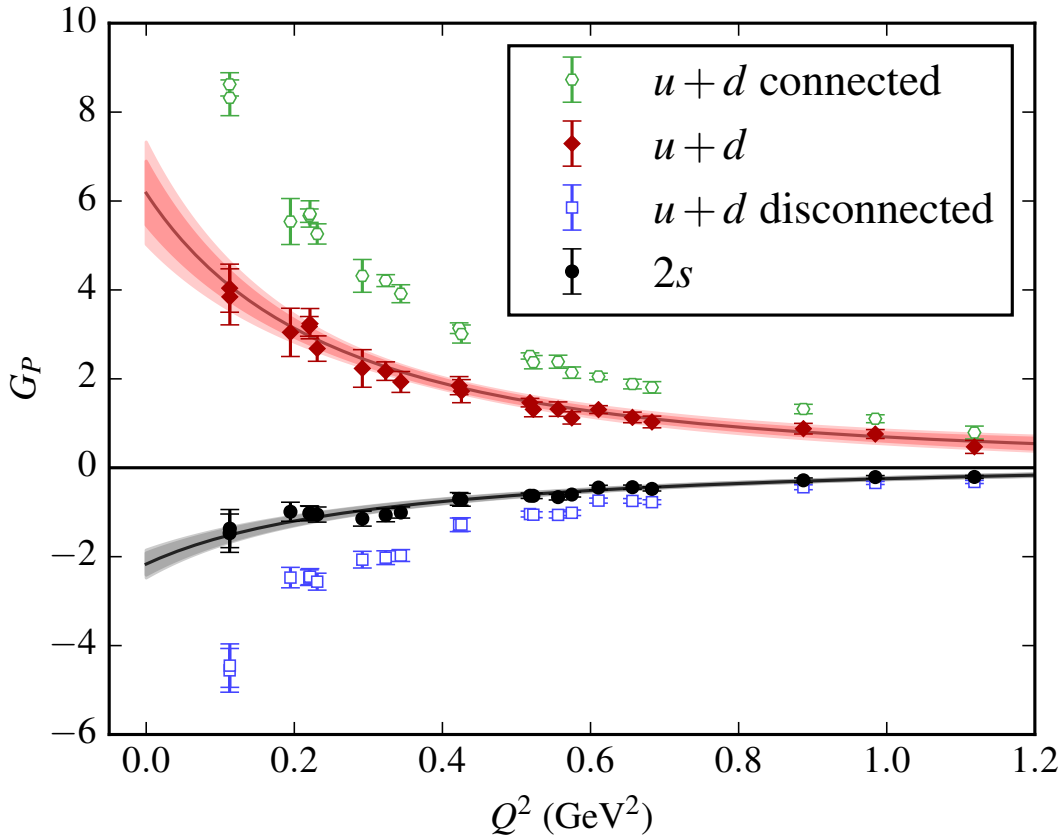

$m_\pi = 317$ MeV.

JG *et al.*, Phys. Rev. D **95**, 114502 (2017) [1703.06703]

Extreme case: isoscalar induced pseudoscalar form factor.

Connected diagrams have pole from partially quenched pion.

Disconnected diagrams must cancel it.

Disconnected diagrams?

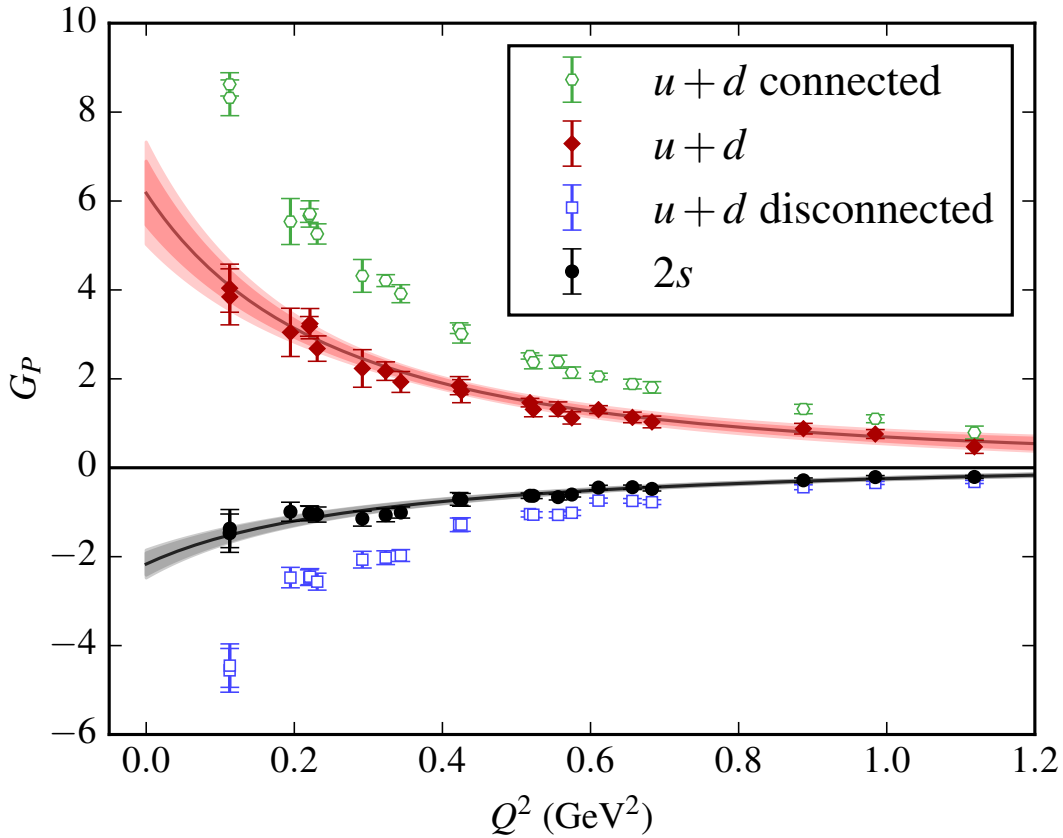

Extreme case: isoscalar induced pseudoscalar form factor.

Connected diagrams have pole from partially quenched pion.

Disconnected diagrams must cancel it.

$m_\pi = 317$ MeV.

JG *et al.*, Phys. Rev. D **95**, 114502 (2017) [1703.06703]

Likewise, disconnected diagrams must cancel $\log(m_\pi)$ term in isoscalar r_E^2.

Disconnected diagrams?

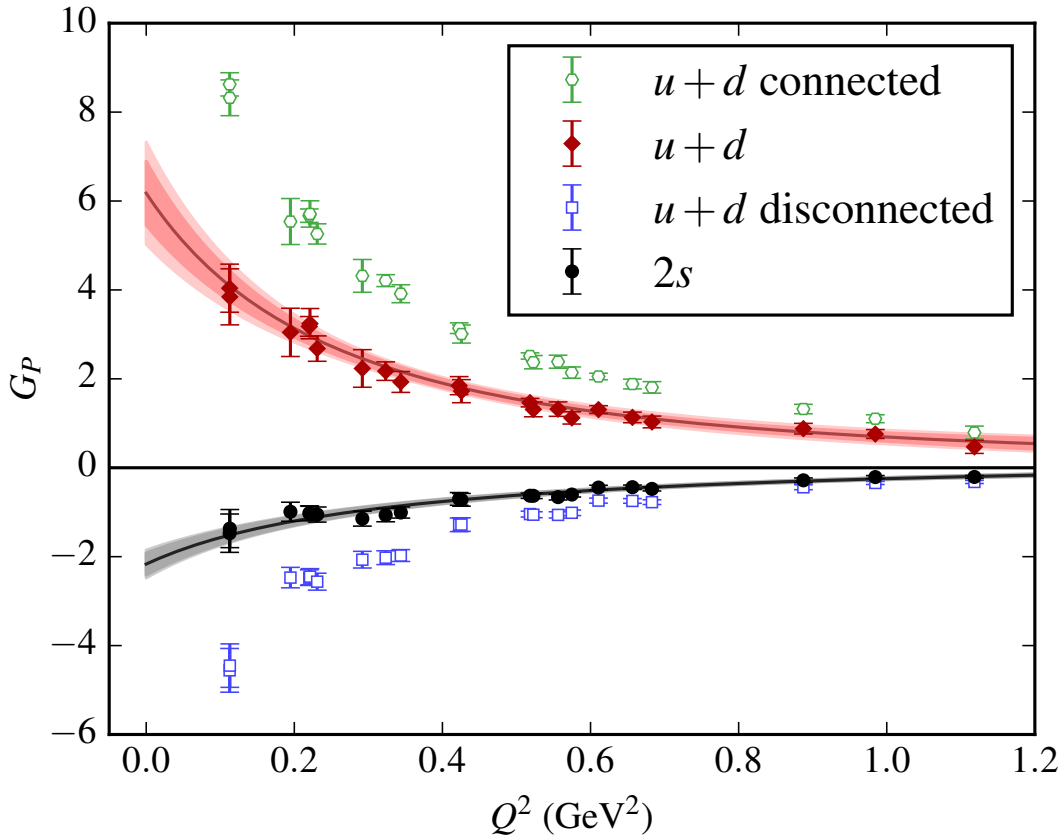

Extreme case: isoscalar induced pseudoscalar form factor.

Connected diagrams have pole from partially quenched pion.

Disconnected diagrams must cancel it.

$m_\pi = 317$ MeV.

JG *et al.*, Phys. Rev. D **95**, 114502 (2017) [1703.06703]

Likewise, disconnected diagrams must cancel $\log(m_\pi)$ term in isoscalar r_E^2.

In practice: contribution is less than 5%. e.g. χQCD, PRD **96**, 114504 [1705.05849]
Large fitting uncertainty is acceptable.

Understanding excited-state effects

Two main models used:

1. "N^* model": well-separated states. Produces OK fits but not very predictive.
2. ChPT: nucleon-pion states. Predictive at leading order but not consistent with data.

Understanding excited-state effects

Two main models used:

1. "N^* model": well-separated states. Produces OK fits but not very predictive.
2. ChPT: nucleon-pion states. Predictive at leading order but not consistent with data.

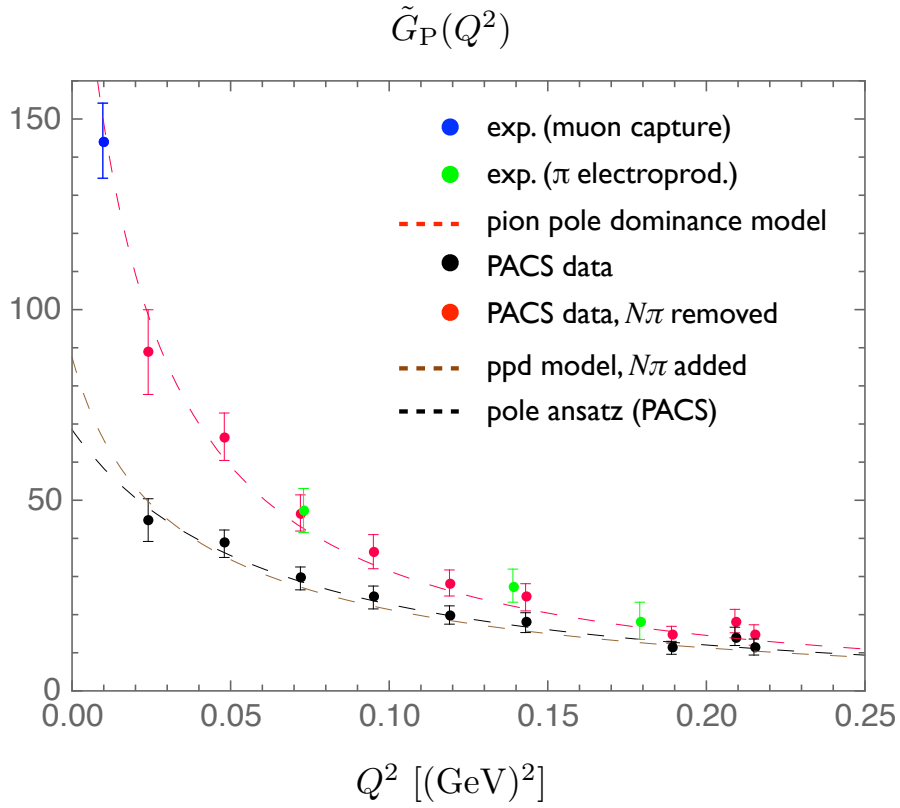

O. Bär, Phys. Rev. D **99**, 054506 (2019) [1812.09191]

Special case: ChPT provides good description for (induced) pseudoscalar form factor. Tree-level diagram dominates.

Understanding excited-state effects

Two main models used:

1. "N^* model": well-separated states. Produces OK fits but not very predictive.
2. ChPT: nucleon-pion states. Predictive at leading order but not consistent with data.

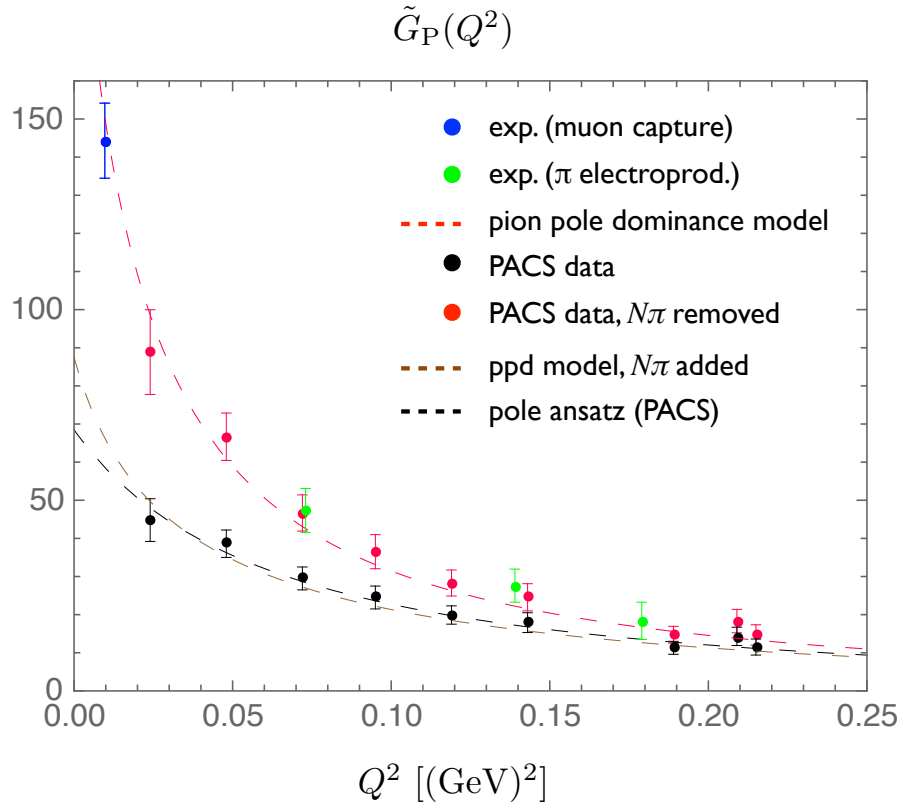

O. Bär, Phys. Rev. D **99**, 054506 (2019) [1812.09191]

Special case: ChPT provides good description for (induced) pseudoscalar form factor. Tree-level diagram dominates.

Speculation:

Could resonance models provide good description of excited-state effects? Are $N\rho$-type states the dominant contribution for G_E and G_M?

Outlook

Derivative method makes it possible to avoid uncertainty in r_E from fitting $G_E(Q^2)$.

- Applies to connected diagrams: largest contribution to r_E.
- Exponentially suppressed finite-volume effects.

Outlook

Derivative method makes it possible to avoid uncertainty in r_E from fitting $G_E(Q^2)$.

- Applies to connected diagrams: largest contribution to r_E.
- Exponentially suppressed finite-volume effects.

Can compare observed volume dependence with ChPT.

- Magnetic moment: same sign, similar size.
- Charge radius: opposite sign, observed effect much smaller.

ChPT: should aim for $m_\pi L \gtrsim 5$ for useful results.

Outlook

Derivative method makes it possible to avoid uncertainty in r_E from fitting $G_E(Q^2)$.

- Applies to connected diagrams: largest contribution to r_E.
- Exponentially suppressed finite-volume effects.

Can compare observed volume dependence with ChPT.

- Magnetic moment: same sign, similar size.
- Charge radius: opposite sign, observed effect much smaller.

ChPT: should aim for $m_\pi L \gtrsim 5$ for useful results.

Excited-state effects remain a significant challenge.